Anal. Chem. **2006,** *78,* 4779−4785

Electrokinetic Protein Preconcentration Using a Simple Glass/Poly(dimethylsiloxane) Microfluidic Chip

Sun Min Kim,[†,‡] Mark A. Burns,[‡,§] and Ernest F. Hasselbrink*[,†]

Department of Mechanical Engineering, Department of Chemical Engineering, and Department of Biomedical Engineering, University of Michigan, Ann Arbor, Michigan 48109-2125

We discovered that a protein concentration device can be constructed using a simple one-layer fabrication process. Microfluidic half-channels are molded using standard procedures in PDMS; the PDMS layer is reversibly bonded to a glass base such as a microscope slide. The microfluidic channels are chevron-shaped, in mirror image orientation, with their apexes designed to pass within ~20 μm of each other, forming a thin-walled section between the channels. When an electric field is applied across this thin-walled section, negatively charged proteins are observed to concentrate on the anode side of it. About 10^3-10^6-fold protein concentration was achieved in 30 min. Subsequent separation of two different concentrated proteins is easily achieved by switching the direction of the electric field in the direction parallel to the thin-walled section. We hypothesize that a nanoscale channel forms between the PDMS and the glass due to the weak, reversible bonding method. This hypothesis is supported by the observation that, when the PDMS and glass are irreversibly bonded, this phenomenon is not observed until a very high E-field was applied and dielectric breakdown of the PDMS is observed. We therefore suspect that the ion exclusion−enrichment effect caused by electrical double layer overlapping induces cationic selectivity of this nanochannel. This simple on-chip protein preconcentration and separation device could be a useful component in practically any PDMS-on-glass microfluidic device used for protein assays.

The development and fabrication of microfluidic systems for analyzing chemical and biological samples has increased dramatically in the past decade.[1−4] Microfluidic systems are used in medical, pharmaceutical, and defense applications, such as drug screening,[5] DNA analysis and sequencing,[2,6] clinical diagnostics,[7] and portable biological/chemical agent detection.[8−10]

One challenge posed by miniaturization of biochemical analysis lies in the detection of very dilute solutions of analytes. Fortunately, there is frequently a much larger volume of sample available than the nanoliter volumes used in microchip-based analysis,[11,12] which suggests the use of enzymatic strategies or sample preconcentration to enhance detector signal.[13,14] Several approaches have been described for the on-chip concentration of proteins and DNA using electrokinetic mechanisms. Singh and co-workers[15] discovered an electrokinetic concentration technique using microcapillaries packed with nanoporous silica particles. Proteins concentrate at the head of such a column when an electric field is applied but can be eluted by pressure-driven flow. Khandurina and co-workers[12,16,17] developed a microfabricated porous membrane structure that enables electrokinetic concentration of DNA and protein samples using homogeneous buffer conditions followed by injection into a channel for electrophoretic analysis. Yu and co-workers[13] fabricated a microfluidic device incorporating monolithic porous polymers prepared by photoinitiated polymerization within the channels and used this device

* To whom correspondence should be addressed. Phone: (734) 355-2879. Fax: (734) 936-0343. E-mail: efhass@umich.edu.

† Department of Mechanical Engineering.

‡ Department of Biomedical Engineering.

§ Department of Chemical Engineering.

(1) Manz, A.; Graber, N.; Widmer, H. M. *Sens. Actuators, B* **1990**, *1*, 244−248.

(2) Burns, M. A.; Johnson, B. N.; Brahmasandra, S. N.; Handique, K.; Webster, J. R.; Krishnan, M.; Sammarco, T. S.; Man, P. M.; Jones, D.; Heldsinger, D.; Mastrangelo, C. H.; Burke, D. T. *Science* **1998**, *282*, 484−487.

(3) Sanders, G. H. W.; Manz, A. *TrAC-Trends Anal. Chem.* **2000**, *19*, 364−378.

(4) Harrison, D. J.; Fluri, K.; Seiler, K.; Fan, Z. H.; Effenhauser, C. S.; Manz, A. *Science* **1993**, *261*, 895−897.

(5) Effenhauser, C. S.; Bruin, G. J. M.; Paulus, A.; Ehrat, M. *Anal. Chem.* **1997**, *69*, 3451−3457.

(6) Schmalzing, D.; Adourian, A.; Koutny, L.; Ziaugra, L.; Matsudaira, P.; Ehrlich, D. *Anal. Chem.* **1998**, *70*, 2303−2310.

(7) Pal, R.; Yang, M.; Lin, R.; Johnson, B. N.; Srivastava, N.; Razzacki, S. Z.; Chomistek, K. J.; Heldsinger, D. C.; Haque, R. M.; Ugaz, V. M.; Thwar, P. K.; Chen, Z.; Alfano, K.; Yim, M. B.; Krishnan, M.; Fuller, A. O.; Larson, R. G.; Burke, D. T.; Burns, M. A. *Lab Chip* **2005**, *5*, 1024−1032.

(8) Vanderschoot, B. H.; Vandenvlekkert, H. H.; Derooij, N. F.; Vandenberg, A.; Grisel, A. *Sens. Actuators, B* **1991**, *4*, 239−241.

(9) Vandenberg, A.; Grisel, A.; Verneynorberg, E.; Vanderschoot, B. H.; Koudelkahep, M.; Derooij, N. F. *Sens. Actuators, B* **1993**, *13*, 396−399.

(10) Anderson, J. R.; Chiu, D. T.; Jackman, R. J.; Cherniavskaya, O.; McDonald, J. C.; Wu, H. K.; Whitesides, S. H.; Whitesides, G. M. *Anal. Chem.* **2000**, *72*, 3158−3164.

(11) Chen, X. X.; Wu, H. K.; Mao, C. D.; Whitesides, G. M. *Anal. Chem.* **2002**, *74*, 1772−1778.

(12) Khandurina, J.; Jacobson, S. C.; Waters, L. C.; Foote, R. S.; Ramsey, J. M. *Anal. Chem.* **1999**, *71*, 1815−1819.

(13) Yu, C.; Davey, M. H.; Svec, F.; Frechet, J. M. J. *Anal. Chem.* **2001**, *73*, 5088−5096.

(14) Song, S.; Singh, A. K.; Kirby, B. J. *Anal. Chem.* **2004**, *76*, 4589−4592.

(15) Singh, A. K., Throckmorton, D. J., Kirby, B. J., Thompson, A. P. *MicroTAS* **2002**, 347.

(16) Khandurina, J.; McKnight, T. E.; Jacobson, S. C.; Waters, L. C.; Foote, R. S.; Ramsey, J. M. *Anal. Chem.* **2000**, *72*, 2995−3000.

(17) Foote, R. S.; Khandurina, J.; Jacobson, S. C.; Ramsey, J. M. *Anal. Chem.* **2005**, *77*, 57−63.

10.1021/ac060031y CCC: $33.50
Published on Web 05/24/2006

for on-chip solid-phase extraction and preconcentration. Ross and co-workers[18−20] achieved concentration of analytes by balancing the electrophoretic velocity of an analyte against the bulk flow of solution in the presence of a temperature gradient. This technique was demonstrated for a variety of analytes, including fluorescent dyes, amino acids, DNA, proteins, and particles, and was shown to be capable of greater than 10^3-fold concentration of a dilute analyte. Recently, Wang and co-workers[21] developed a protein preconcentrator based on an electrokinetic trapping mechanism enabled by a nanofluidic filter. They achieved a high concentration rate and up to 10^6-10^8 increase in concentration overall. Normal and tangential electric fields to the nanofilter must be carefully controlled to achieve protein concentration.

It is important to note that the above work has suggested several mechanisms for preconcentration. Unfortunately, due to the inherent difficulties of measuring fluid velocities in nanochannels, in most cases, the hypothesized mechanisms are not yet substantiated by conclusive data (this is not to criticize the above works' efforts to do so; indeed the present work falls short in this regard as well). Many of these devices require a special buffer system or reagents to achieve concentration. Also, the reproducibility is difficult in a device that has a nanoporous thin-walled section or packed nanosilica particles inside a microchannel due to fouling.

In this present work, the main contribution is to report a device that can achieve as high as 10^6-fold concentration in ~30 min, comparable or better in performance to the microdevices described above, but one that is extraordinarily easy to construct. After considering several possible explanations of the concentration mechanism, our data best support the hypothesis that this is an exclusion−enrichment effect (EEE) of the nanochannel combined with electrokinetic transport of the protein.

EXPERIMENTAL SECTION

Materials. Phosphate-buffered saline (PBS; 10 mM, pH 7.4) and phosphate buffer (20 mM, pH 7.2) solution were used for the buffer system. Fluorescein isothiocyanate conjugate bovine serum albumin (BSA) (Sigma-Aldrich, St. Louis, MO) and ovalbumin (Molecular Probes, Eugene, OR) were used for on-chip preconcentration and separation experiments, and each protein was diluted with the buffer solution at different concentrations (100 nM, 10 nM, 100 pM, and 1 pM). Cationic Rhodamine 123 dye (Molecular Probes) was used to show the analyte charge effects on the concentration phenomena. All protein samples were kept in a freezer to prevent deterioration, and all liquid samples were filtered with a 0.2-μm syringe filter (Whatman, Maidstone, UK) to remove particulates.

Microchip Fabrication. The microchannel system in Figure 1 was fabricated by casting poly(dimethylsiloxane) (PDMS) over an SU-8 photoresist (SU 8-2010, MicroChem Inc., Newton, MA) mold on a silicon substrate fabricated by photolithography as previously described.[10,22−27] Briefly, a 10:1 weight ratio mixture of the PDMS prepolymer and the curing agent (Sylgard 184, Dow Corning, Midland, MI) was prepared using a typical electric hand mixer and placed in a vacuum to evacuate any bubbles created during mixing. The uncured mixture was poured over the mold in a Petri dish and cured following the conditions recommended by the manufacturer (24 h at room temperature, 6 h at 60 °C, and 1 h at 150 °C) until cured. The cured PDMS was detached from the Petri dish and 2-mm-diameter holes for reservoirs were punched vertically through. Cylindrical glass reservoirs (2 cm long, 5-mm i.d., 7-mm o.d.) were bonded concentrically over the holes using UV-curable optical adhesive (Norland, New Brunswick, NJ) with a UV lamp for 10 min. Three different bonding methods for binding a PDMS slab on a substrate were employed to obtain different bonding strengths:[11,24,28] (a) The PDMS slab with the designed microchannel pattern was placed in contact with a microscope slide and treated with an air plasma of 100-W RF power in ~300 mTorr vacuum using a PlasmaPrepII system (SPI supplies, West Chester, PA) for 3 min. This bonding procedure produces a "reversible" bonding between the PDMS and a glass substrate that can be easily peeled apart; however, no leakage of fluids is observed from the channel. (b) The PDMS slab and a slide glass were treated with air plasma first, and then contacted together, followed by heating at 150 °C for 15 min. This procedure creates an "irreversible" bond between the PDMS slab and a glass substrate, insofar as that the bond cannot be peeled apart without damaging the bulk PDMS. (c) The PDMS slab with channels,

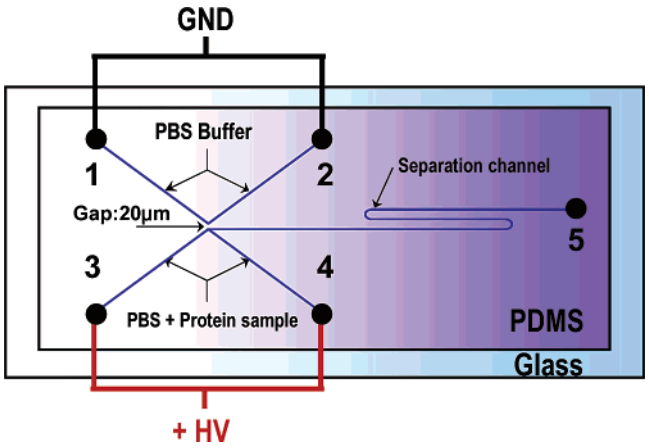

Figure 1. PDMS thin-walled section protein concentration device and electrical configuration for concentration process. Top and bottom channels are 20 μm apart from each other. The top channel is filled with PBS buffer solution (pH 7.4), and the bottom channel is filled with a mixture of protein sample and PBS buffer solution. Electrical field is applied across the top and bottom channels (V_1, V_2, ground; V_3, V_4, + high voltage) while port 5 is float. The dimensions of each top and bottom channels are 40-μm width, 18-μm depth, and 16-mm length. The dimensions of the separation channels are 30-μm width, 18-μm depth, and ~4-cm length.

(18) Ross, D.; Locascio, L. E. *Anal. Chem.* **2002**, *74*, 2556−2564.
(19) Balss, K. M.; Vreeland, W. N.; Howell, P. B.; Henry, A. C.; Ross, D. *J. Am. Chem. Soc.* **2004**, *126*, 1936−1937.
(20) Balss, K. M.; Vreeland, W. N.; Phinney, K. W.; Ross, D. *Anal. Chem.* **2004**, *76*, 7243−7249.
(21) Wang, Y. C.; Stevens, A. L.; Han, J. Y. *Anal. Chem.* **2005**, *77*, 4293−4299.
(22) Kumar, A.; Whitesides, G. M. *Appl. Phys. Lett.* **1993**, *63*, 2002−2004.
(23) McDonald, J. C.; Chabinyc, M. L.; Metallo, S. J.; Anderson, J. R.; Stroock, A. D.; Whitesides, G. M. *Anal. Chem.* **2002**, *74*, 1537−1545.
(24) McDonald, J. C.; Duffy, D. C.; Anderson, J. R.; Chiu, D. T.; Wu, H. K.; Schueller, O. J. A.; Whitesides, G. M. *Electrophoresis* **2000**, *21*, 27−40.
(25) McDonald, J. C.; Metallo, S. J.; Whitesides, G. M. *Anal. Chem.* **2001**, *73*, 5645−5650.
(26) Folch, A.; Ayon, A.; Hurtado, O.; Schmidt, M. A.; Toner, M. *J. Biomechan. Eng.−Trans. ASME* **1999**, *121*, 28−34.
(27) Kumar, A.; Biebuyck, H. A.; Whitesides, G. M. *Langmuir* **1994**, *10*, 1498−1511.
(28) Duffy, D. C.; McDonald, J. C.; Schueller, O. J. A.; Whitesides, G. M. *Anal. Chem.* **1998**, *70*, 4974−4984.

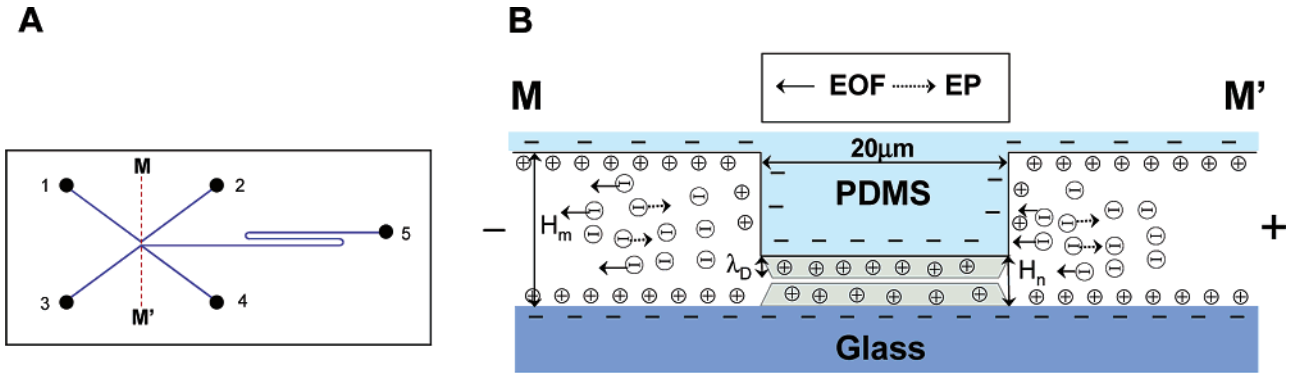

Figure 2. Electrokinetic preconcentration mechanism. (A) Schematic diagram of the microchannel system, which shows the position of cross section M−M′. (B) The cross-sectional view of near the PDMS thin-walled section. We hypothesize here weak bonding between the PDMS thin-walled section (20-μm width) and the glass substrate creates a nanochannel. The depth of the nanochannel (H_n) is comparable to the electrical double layer (EDL, λ_D) thickness of the charged surfaces, such that the EDL of top and bottom surfaces can be overlapped. The EDL overlapping results in electrostatic effects on the ions in the nanochannel. Co-ions are excluded from the nanochannel, whereas counterions are enriched in the nanochannel to ensure the overall electroneutrality of the nanochannel (EEE). The negatively charged protein at the anode side cannot easily pass through the nanochannel between the PDMS thin-walled section and a glass substrate due to the cation selectivity of the nanochannel and thus can be concentrated at the entrance of the nanochannel due to the higher elecroosmotic flux by applied external electric potential.

and a flat PDMS substrate, both of which have a slightly off-stoichiometric ratio of PDMS prepolymer and curing agent, are contacted together as described by Unger et al.[29] These were then treated with air plasma and contacted together. The structure was heated following the same conditions in (b), resulting in irreversibly bonded microchannels with homogeneous wall surface material.

Instrumentation and Electrical Setup. The protein concentration was monitored by an inverted fluorescence microscopic system (IX-71, Olympus) equipped with a spectral filter set for FITC (488 nm) and a 100-W mercury lamp. A charge-coupled device camera (Hamamatsu) was mounted on the microscope for image acquisition, and IPLab 3.6 software (Scanalytics, Fairfax, VA) was used for camera control and image processing. To prevent photobleaching of FITC, a neutral density filter (ND 1.0, Omega Optical, Brattleboro, VT) was installed to reduce excitation light intensity, and using a shutter, the system was exposed to excitation only during image capture (~2 s). A high-voltage power supply (PS350, Stanford Research Systems, Sunnyvale, CA) was used to apply electric fields to the microchannel through bright platinum electrodes placed in the reservoirs, and a custom-built rack of relays (G10C, Gigavac, Santa Barbara, CA) was used to switch the electric field for preconcentration and separation. A photomultiplier tube (PMT) (model H8568-02, Hamamatsu) system, also connected to the side port of the microscope, was used to detect the separated peaks of the protein samples. All system operations were performed with Labview 7.1(National Instrument, Austin, TX) programmed through a PC-based computer equipped with a DAQ board (PCI 6014, National Instrument).

For reliable quantification of the protein concentration, nearly all experiments were performed with a fresh new device. In certain experiments, wherein the aim was to reduce nonspecific binding of labeled protein on the channel surface, "used" devices were employed so that the surface was already heavily coated with protein. In these experiments, the protein-concentrated region had been exposed with laser light (~495 nm) to thoroughly bleach the fluorescence. Background noise correction was performed with a pure dark image, and a flat-field correction (to correct for the distribution of illumination intensity from the UV lamp) was obtained by imaging fluorescence of a Schott colored glass filter (model CG-520, Newport Corp., Irvine, CA).

RESULTS AND DISCUSSION

Electrokinetic Concentration and Separation of Protein. Electrokinetic protein concentration was achieved near the thin PDMS "thin-walled section" as shown in Figure 1. A cross-sectional view in Figure 2 shows the microchannel cross sections, and what we hypothesize (with an exaggerated height in the figure) is a narrow channel underneath the wall (between the PDMS and glass) through which ionic transport can occur if a sufficient E-field is applied. The depth of this hypothetical nanochannel between the PDMS and glass substrate might be only on the order of 1 nm and the size and characteristics of these nanochannels are controlled via different bonding methods of the PDMS with substrate. Differences observed using different bonding approaches will be described later.

To operate the device, the top microchannel is filled with the PBS buffer solution and the bottom channel is filled with a 10 nM FITC-labeled BSA in PBS buffer solution, and then voltages are applied at ports 1−5 (as given in Figure 1) as V_1, V_2 = ground, V_3, and V_4 = 200 V, while port 5 is left floating. As shown in Figure 3, the negatively charged FITC-labeled BSA proteins are concentrated near the anodic electrode side (bottom channel) PDMS thin-walled section as expected. The protein concentration experiments were continued for 30 min to verify the stability of the concentration process. No unstable phenomena were observed, and once the concentration step was finished, it was possible to inject protein into a separation channel (separation of BSA and OVA protein mixture sample will be shown in a later section.). Protein concentration experiments were performed with three different initial concentration FITC BSA samples (1 pM, 100 pM, 10 nM). Fluorescence intensity was averaged over a measurement

(29) Unger, M. A.; Chou, H. P.; Thorsen, T.; Scherer, A.; Quake, S. R. *Science* **2000**, *288*, 113−116.

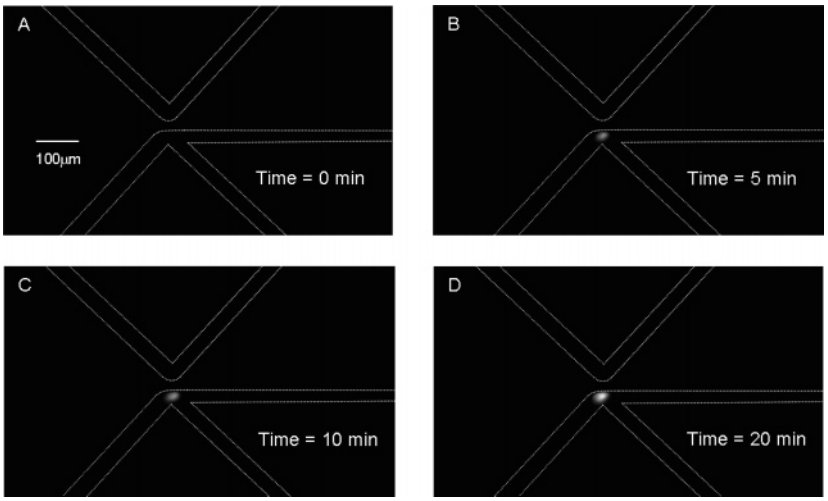

Figure 3. Time sequence images of concentration of FITC-labeled BSA in the PDMS microchannel with a reversibly bonded glass. (A) Image taken before electric field is applied. Top channel is filled with PBS buffer solution, and bottom channel is filled with 10 nM BSA in PBS buffer solution (pH 7.4). (B−D) Images taken after applying V_1, V_2 = ground and V_3, V_4 = 200 V while port 5 is float for 5, 10, and 20 min, respectively.

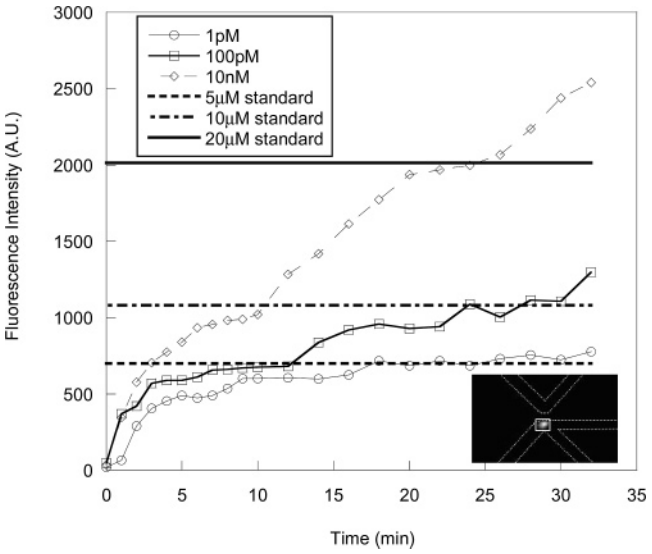

Figure 4. Concentration of FITC-labeled BSA with same voltage configuration in Figure 3. Three different initial concentration samples are presented. Concentrations of each sample are compared with standard concentration samples (5, 10, and 20 μM). About 10^3-10^6-fold concentration achieved in 30 min. Fluorescence intensity was averaged over a measurement window specified by the rectangle in the inset.

window specified with the rectangle in the inset of Figure 4 and compared with the fluorescence intensity of the standard sample solutions (5, 10, and 20 μM). The fluorescence intensity increased up to 10^3-10^6-fold of the initial concentrations at the concentration region in 30 min quite stably.

This observation led to the development of several hypotheses for the concentration mechanism; one that remains particularly intriguing is the "exclusion−enrichment effect". It is well known that PDMS and glass nanochannels have charge selectivity induced by surface charge.[21,30−33] The thickness of the electrical double layer (λ_D, EDL in Figure 2B) is usually on the order of 1−10 nm[34] for 1−100 mM ionic strengths (assuming singly valent counterions), and so as shown in Figure 2B, the EDL of the hypothetical nanochannel(s) between the PDMS thin-walled section and substrate may be overlapped since H_n is comparable to λ_D. For a negatively charged surface, the potential within the channel, compared to an electroneutral solution, is negative; therefore, anions (co-ions) are excluded from the nanochannel, whereas cations (counterions) are enriched in the nanochannel to ensure the overall electroneutrality of the nanochannel (recently this effect has been called the EEE).[31−33] That is, a nanochannel with negatively charged surfaces acts as a cation-selective thin-walled section, and inversely for positively charged surfaces.

In our case, PDMS and glass are both negatively charged at near-neutral pH, and so the nanochannel formed between the PDMS thin-walled section and glass substrate has cationic selectivity due to the negative charge of the channel surfaces. Thus, negatively charged proteins are excluded from the entrance of the nanochannel and cannot easily pass through it. However, the electric field applied through the whole channel network (micro- and nanochannels in series) causes electroosmotic flow (EOF), which, under the right conditions, dominates over electrophoresis. Thus, protein molecules in the anode side microchannel are transported by higher EOF through the microchannel toward the nanochannel. However, once they arrive there, they are preferentially excluded from passing through the nanochannel by the EEE, and thus they accumulate near the micro-/nanochannel junction. Such a mechanism of concentration of protein in a device combining micro- and nanochannels was reported by Wang et al. with ion-selective thin-walled section effects and electrokinetics of the second kind,[21] but the present device appears to be much easier to construct and operate.

(30) Petersen, N. J.; Dutta, D.; Alarie, J. P.; Ramsey, J. M. In *Micro Total Analysis Systems 2004*; Laurell, T., Nilsson, J., Jensen, K., Harrison, D. J., Kutter, J. P., Eds.; Royal Society of Chemistry: Cambridge, UK, 2004; Vol. 1, pp 348−350.

(31) Pu, Q. S.; Yun, J. S.; Temkin, H.; Liu, S. R. *Nano Lett.* **2004**, *4*, 1099−1103.

(32) Plecis, A.; Schoch, R. B.; Renaud, P. *Nano Lett.* **2005**, *5*, 1147−1155.

(33) Plecis, A.; Schoch, R. B.; Renaud, P. In *Micro Total Analysis Systems 2005*; Royal Society of Chemistry: Cambridge, UK, 2005; Vol. 1, pp 1038−1040.

(34) Probstein, R. F. *Physicochemical hydrodynamics: an introduction*; John Wiley & Sons: Inc.: New York, 1994.

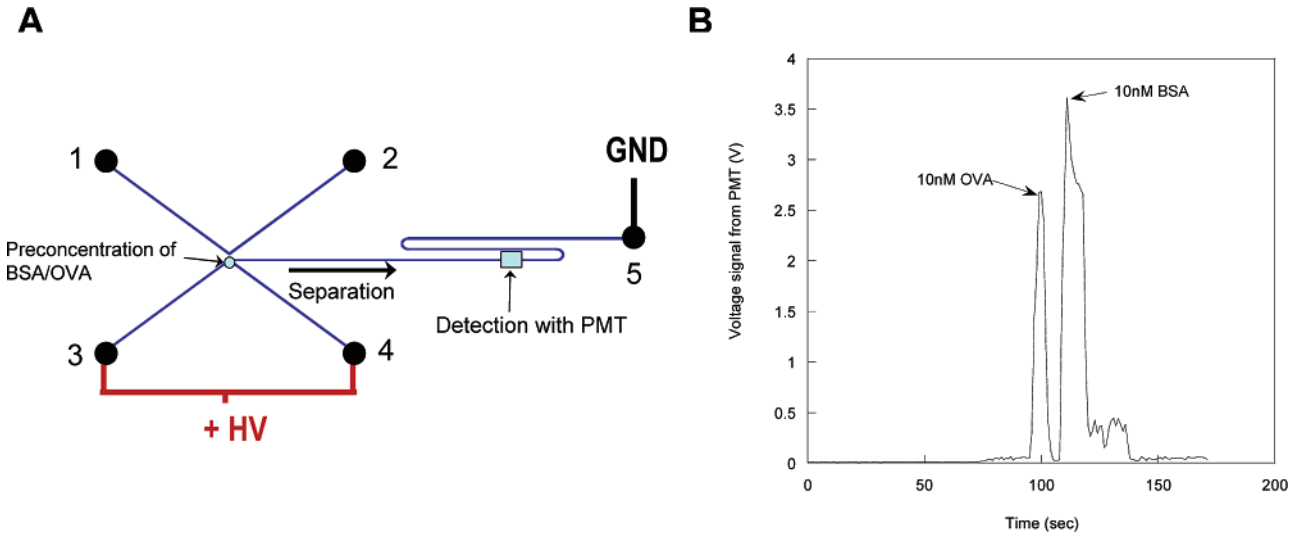

Figure 5. Electrophoretic separation of preconcentrated protein mixture. (A) Mixture of 10 nM BSA and 10 nM OVA in PBS buffer solution is concentrated by 200 V with concentration voltage configuration for 15 min, and separation of concentrated proteins is achieved by applying V_3, V_4 = 600 V and V_5 = ground, while ports 1 and 2 are float. (B) Separation of proteins is detected with PMT downstream in the separation channel. Electropherogram shows two sharp peaks of BSA and OVA.

An interesting phenomenon observed during this concentration process is that the rate of concentration is noticeably decreased when the concentration exceeded ~3 μM as shown in Figure 4. One possible cause of this phenomenon is nonspecific binding of the protein on the channel surface as described in previous research.[21] Furthermore, it appears that the concentration factors may be leveling off once the concentration factor reaches a certain level (e.g., the 1 pM sample signal appears to be leveling off at a signal equivalent to a concentration of 5 μM).

We also note that the 1 pM sample, is concentrated to an apparent concentration of 5 μM in a region occupying ~30 pL (~40 μm × 40 μm × 18 μm) in 30 min. This 5 × 10^6-fold concentration factor requires that protein molecules that originally occupied ~150 μL of buffer solution (~25% of total volume of sample solution in the reservoirs and channel of anode side) must have aggregated at the membrane. This is surprising, but not impossible; however, the fact that a 150-μL flux occurred in 30 min implies that the average electrophoretic speed through the microchannels is 5 cm/s (recalling that we have two channels in parallel feeding the membrane). This seems quite extraordinary, since this high flow speed is not possible with typical electroosmotic flow (~600 μm/s with 200 V). A recent paper by Wang et al. claims that high flow speed can be explained by electroosmotic flow of the second kind, which causes an electroosmotic flow nonlinear to the applied electric field,[21,35] and indeed, their data appear to imply similar high-speed transport in similar microchannels. However, they imply speeds of 1 mm/s or so, which is still a factor of 50 below the ones implied above.

This observation increased our skepticism about whether the observed signal enhancement was real or if perhaps other contaminants were aggregating at the concentration spot. We therefore conducted separation experiments by switching the direction of the electric field as shown in Figure 5 (A). Our photomultiplier tube was first calibrated against a standard solution (by filling a channel of an identical "calibration" microchannel with solution, measuring the fluorescence, and then discarding the calibration device—thus ensuring no contamination). Figure 5B shows a typical resulting separation of two different protein species (BSA and ovalbumin, OVA). In this experiment, the preconcentration step was performed for 15 min and the separation was quite clearly achieved in 2 min. We note that, with the particular setup and PMT gain used in this experiment, if we fill the channel with 10-nm protein solution, the signal is below the LOD. However, after concentration, the signal is quite clear. As a more quantitative comparison, we present two plots in the supporting online information that show 1 and 10 pM sample electrophoresis runs, which show signal comparable to that obtained by filling the channel with a 100 nM solution, implying 10^4−10^5-fold signal enhancement. As per the discussion above, these imply a few millimeter per second drift speeds in the microchannel, which seems difficult to believe. It is possible that some other change (e.g., spectroscoping properties or some kind of thermal phenomenon caused by Joule heating at the concentration spot) is occurring that enhances the signal, but we have not uncovered it. Therefore, at this point, we do not have conclusive evidence that the concentration has actually increased by factors of 10^5 or so, but we have verified that detectability can be enhanced by this much. We strongly suspect that a large factor of concentration is occurring but that the signal might be enhanced even further by some other mechanism.

Further Experimental Investigation of the Concentration Mechanism. To investigate the hypothesis of an electrokinetic protein concentration mechanism with ion exclusion and enrichment effects and ionic selectivity of the nanochannel formed between the PDMS thin-walled section and the substrate, two additional experiments were performed. The first is that the same protein concentration experiments were performed with the top and the bottom channels filled entirely with the 100 nM FITC BSA sample. This experiment was performed to verify the hypothesis that the concentration occurs only on one side, implying that the electroosmotic flow velocity is faster than the

(35) Mishchuk, N. A.; Takhistov, P. V. *Colloids Surf., A* **1995**, *95*, 119−131.

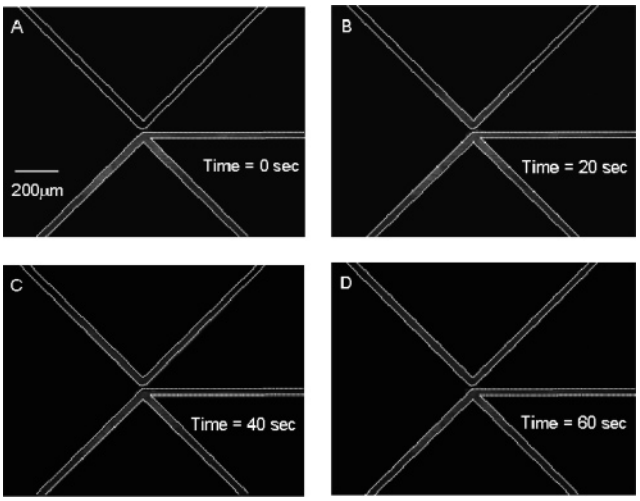

Figure 6. Time sequence images of concentration experiment with Rhodamine 123 dye (cationic dye) in PBS buffer solution. (A) Image taken before electric field is applied. Top channel is filled with PBS buffer solution, and bottom channel is filled with 1 μM Rhodamine 123 dye in PBS buffer solution. (B−D) Images taken after applying V_1, V_2 = ground and V_3, V_4 = 200 V for 20, 40, and 60 s, respectively. The dye solution of the bottom channel flowed through the nanochannel between PDMS thin-walled section and glass substrate. This result shows the cation selectivity of the nanochannel.

electrophoretic velocity of the protein, and the protein molecules in the cathodic side channel can freely move to the cathode. The initial concentration of sample for this experiment is higher than the concentration used for previous experiments to observe the concentration change of both channels. The applied electric field strength and configurations are the same as those in Figure 3. As we expected, the protein concentration was observed only in the bottom anode side channel with the same manner in Figure 3 (see Supporting Information). In terms of our previously described hypothesis, the negatively charged protein molecules are excluded from the nanochannel by the cationic-selective characteristic of the nanochannel, but the concentration occurs on the anode side because electroosmotic flow dominates electrophoresis. In contrast, the excluded protein molecules on the cathode side move toward the cathode side freely without any obstruction (see Supporting Information). We furthermore attempted putting protein solution only on the cathode side, and indeed, none appears on the anode side of the membrane (see Supporting Information).

The second experiment for the verification of this hypothesis was performed with positively charged Rhodamine 123 dye in PBS buffer solution. This experiment was performed to verify the cationic selectivity of the nanochannel between the PDMS thin-walled section and the substrate. The top channel was filled with PBS buffer solution, and the bottom channel was filled with 1 μM Rhodamine 123 dye in PBS buffer solution. The applied electric field strength and configurations are the same as those in Figure 3. As shown in Figure 6, the positively charged dye quickly passed through the PDMS thin-walled section and moved toward the cathode. This result confirms the cationic selectivity of the nanochannel formed between the PDMS thin-walled section and the substrate. In addition, both the electrophoresis of the positively charged dye molecules and the bulk electroosmosis move in the same direction, so the positively charged dye molecules move much faster than the negatively charged molecules.

In summary, the two experiments explained in this section can explain the EEE of ions and the cationic selectivity of the nanochannel by EDL overlapping. If the channel surfaces are modified to be positively charged surfaces, the nanochannel might have the anionic selectivity and positively charged molecules can be collected near the thin-walled section in the same manner.

Electric Field Strength Effects on the Protein Concentration. The electric field strength applied to this microfluidic system is an issue because the cross-sectional area of the microchannel is much bigger than that of the nanochannel formed between the PDMS thin-walled section and the substrate; the depth of the microchannel is ~18 μm but the depth of nanochannel might be only on the order of nanometers. Due to this significant dimensional difference, Joule heating could be expected to be problem at the nanochannel, where the E-field is highest. Four different voltages were applied to the channel system to show the electric field strength effects on the protein concentration: 50, 100, 200, and 300 V.

Well-maintained protein concentrations were achieved with 100 and 200 V. However, no protein concentration was observed when applying 50 V, and bubbles were observed when applying 300 V, suggesting boiling. Since Joule heating is proportional to the square of E-field strength, we might expect that if 300 V is required to commence boiling (heating the solution by ~75 °C), 200 V might be heating the solution by as much as $(200/300)^2 \times 75$ °C = 33 °C and in the 100 V case should only be heating the solution by ~8 °C.

One might hypothesize that, for a fixed geometry device of this sort, the rate of protein concentration might be linearly proportional to the voltage applied, because of the linear relationship between EOF and electrophoresis with E-field. However, this overlooks significant increases in mobility that can occur with fairly modest changes in temperature; in fact, we might expect somewhat faster concentration at higher voltages. The experimental data confirm that this trend is observed: protein concentration is plotted versus the product of time and voltage in Figure 7 (this experiment was performed with 10 nM FITC BSA and the same electrical configuration as Figure 1). The experimental results exhibit a higher rate of concentration when 200 V is applied to the channel than when 100 V is applied. This nonlinear increase of the concentration of sample in a microdevice with nanoporous thin-walled sections, filters, and nanochannels was reported by several research groups, but the mechanism has not yet been fully explained.[12,16,17,21] Furthermore, while this observation supports the EEE hypothesis, it does not rule out other hypotheses (e.g., that this effect is due to temperature gradient focusing[18−20]). Despite the nonlinear increase in concentration, the higher rate and fast protein concentration can be achieved quite stably in this PDMS thin-walled section device.

Bonding Strength Effects on the Protein Concentration. The bonding strength can affect the formation of the nanochannel between the PDMS thin-walled section and the substrate. The PDMS thin-walled section can be bonded with a flat substrate reversibly or irreversibly.[11,24,28] Reversible bonding is possible because cured PDMS is flexible and can be attached to the substrate via van der Waals contact with the substrate. Reversible

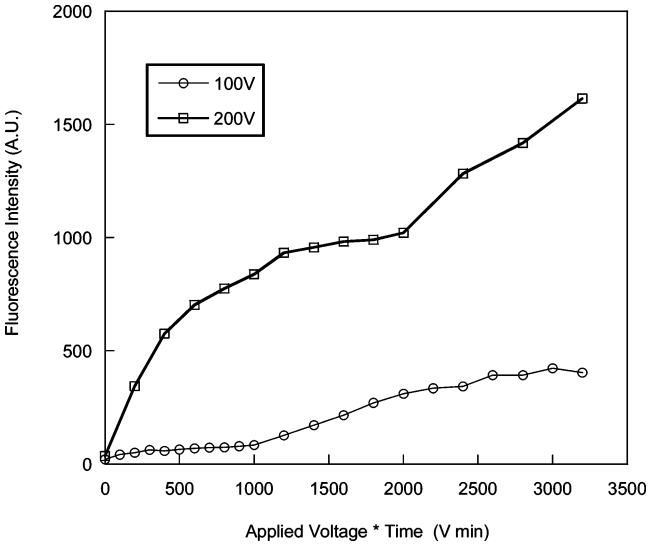

Figure 7. 10 nM FITC-labeled protein concentration profile with different applied voltages. The concentrations of protein by different applied voltages are not the same at the same product of applied voltage and time. With higher voltage, faster and higher concentration is achieved. However, the boiling of sample solution and electrical breakdown through the PDMS thin-walled section occurred at voltages higher than 200 V.

bonding of PDMS cannot withstand high pressures (>5 psi) inside the channel and can be easily broken by peeling off PDMS from the substrate.[24] Irreversible bonding is achieved by exposing a PDMS to air plasma, which introduces polar groups on the surface. When this plasma-treated PDMS makes a conformal contact with a glass or another PDMS slab treated in thewith same manner, a covalent bonding between the PDMS and the substrate is formulated, and this bonding forms a tight and irreversible bond. This bond can withstand pressures of 30−50 psi.

Three different bonding methods are examined for the concentration of protein: (1) reversible bonding of PDMS to a glass substrate, (2) irreversible bonding of PDMS to a glass substrate, and (3) irreversible bonding of PDMS to a PDMS substrate. The protein concentration experiments were performed with FITC BSA samples and the same electrical configuration as previous concentration experiments. In both irreversibly bonded PDMS devices, protein concentration was not achieved with the same applied voltage as the high rate of concentration was achieved in the reversibly bonded PDMS device. The current through the channel in the irreversibly bonded device (~0.003 mA at 200 V) was much lower than that in the reversibly bonded device (~0.02 mA), which can show that the electric and fluidic resistance is too high to achieve the effective electroosmotic flow in the irreversibly bonded device. When 300 and 400 V were applied, the concentration of protein molecules was quite unstable and uncontrollable.

CONCLUSION

A simple microfluidic system for protein preconcentration and separation is developed and investigated. The advantages of this system are a simple fabrication process, a high concentration, and a fast concentration speed; we achieved ~10^3−10^6-fold concentration in 30 min. The nanochannel formed between a PDMS thin-walled section and a glass substrate by reversible bonding plays an important role in this system as a cationic selective thin-walled section. The ion EEE of a nanochannel, combined with the electrokinetic effect of charged protein molecules (including electroosmotic flow and electrophoresis) can explain the concentration mechanism of the negatively charged protein molecules near the PDMS thin-walled section on the anodic channel side. This hypothesis was verified with supporting experiments performed with positively charged Rhodamine 123 dye solution.

The physical mechanism of the protein concentration in this manner is still under investigation; however, temperature gradient focusing (TGF) of the protein molecules by the temperature variations inside the microchannel caused by Joule heating effect can be one possible explanation.[18] TGF relies on the fact that the mobility of the protein molecules depends on the temperature, and the movement of the protein molecules by electrophoresis is balanced with the bulk flow (electroosmotic flow and pressure-driven flow) in the opposite direction. If EOF and electrophoresis have different temperature dependencies, protein molecules can be concentrated where the net velocity of the protein molecules reaches zero (and the flux vector has negative divergence). Thus, TGF may play an important role in all of our devices, since we have observed boiling at voltages of only 3 × 100 V, the lowest voltage by which the concentration was achieved. Since Joule heating is proportional to the square of E-field strength, we might expect that if 300 V is required to commence boiling (heating the solution by ~75 °C), 200 V might be heating the solution by as much as 33 °C. However, our 100-V case should only be heating the solution by ~8 °C, so it seems difficult to explain this high rate of concentration as being only due to TGF.

The key factors for stable concentration with this device are the applied electric field strength and the bonding strength between PDMS and a substrate. Too high electric field strength induces a dielectric breakdown of PDMS thin-walled section and a bubbling problem by Joule heating. In an irreversibly bonded PDMS device, the stability of the concentration is not guaranteed. This device also shows the capability to separate a mixture of several protein species co-concentrated near the PDMS thin-walled section. This on-chip protein preconcentration and separation device would be a useful component of a fully integrated micro total analysis system for biochemical samples.

ACKNOWLEDGMENT

The authors acknowledge National Institute of Dental and Craniofacial Research (Grant 1 U01 DE14961-01) for funding this project. Many helpful discussions with Mr. Greg Sommer are also acknowledged.

SUPPORTING INFORMATION AVAILABLE

Additional information as noted in text. This material is available free of charge via the Internet at http://pubs.acs.org.

Received for review January 6, 2006. Accepted April 21, 2006.

AC060031Y